

Fundamental steps towards interface amorphization during silicon oxidation: Density functional theory calculations

A. Hemeryck,¹ A. Estève,¹ N. Richard,² M. Djafari Rouhani,^{1,3} and Y. J. Chabal^{4,*}

¹CNRS; LAAS; Université de Toulouse, 7 avenue du colonel Roche, F-31077 Toulouse, France

²CEA-DAM-DIF, Bruyères-le-Châtel, 91297 Arpajon Cedex, France

³Université de Toulouse; UPS, INSA, INP, ISAE, LAAS; F-31077 Toulouse, France

⁴Department of Materials Science & Engineering, University of Texas at Dallas, Richardson, Texas 75080-3021, USA

(Received 17 August 2008; revised manuscript received 17 November 2008; published 16 January 2009)

Density functional theory calculations reveal a two-step scenario for silicon oxidation nucleation. We detail a quasibarrierless semihexagonal oxide nucleus, involving an unexpected adjacent dimer oxygen bridging bond. It is formed upon O₂ chemisorption at 0.5 monolayer on Si(100)-(2 × 1). This structure arises from the difficulty to systematically insert oxygen atoms into first neighbor Si–Si bonds. While silanone structures, characterized by a Si=O strand, effectively accommodate oxygen at lower coverages, the stabilization of this hexagonal-like pattern on a cubic substrate at low temperatures and at higher coverages demonstrates the ability of oxygen atoms to deeply modify the arrangement of silicon atoms on the surface and to impose a specific structure. It is believed to offer a key natural pathway toward the formation of an abrupt *crystalline semiconductor/amorphous oxide* transition.

DOI: 10.1103/PhysRevB.79.035317

PACS number(s): 68.35.-p, 68.55.A-, 79.60.Jv

I. INTRODUCTION

One of the greatest technological wonder and scientific puzzle of the past 50 yrs is the quality of the silicon/silicon oxide interface. Its interface state density is remarkably low ($<10^{10}$ cm⁻²), indicating that dangling bonds are fewer than 1 in 10 000,^{1,2} yet the oxide is not crystalline and not commensurate. This system is therefore the ultimate model of *amorphous* thin-film growth and interface quality with a crystalline substrate. It embodies the issues related to order/disorder transitions in heterogeneous systems.

The particular issue of Si/SiO₂ has been reconsidered with the need to replace SiO₂ with high-*k* materials for new generation complementary metal-oxide semiconductor (CMOS) transistors.³ The chemical mechanisms of silicon oxidation and the resulting atomic arrangement at the Si/SiO₂ interface are still far from being understood.^{4,5} There are controversies as to the local order of the interface itself, with suggestions of partial order^{6,7} and evidence for complete disorder.⁸ Since the nature of the Si/SiO₂ interface (even for Si/high-*k* systems where interfacial SiO₂ is also observed⁹) is believed to control most of the electrical properties of Si-based devices, understanding its formation is essential. While there have been numerous theoretical calculations of Si oxidation, most studies have been limited either to structural investigations of oxide structures^{10–12} or to restricted O₂ chemisorption paths on Si(100),^{13–17} making it difficult to reveal the overall mechanistic routes leading to optimum interface configurations. The former approach has brought some structural rules, in particular Yamasaki's work,¹² which identifies oxygen specific sites that are necessary to the oxide stability onto silicon. The second approach addresses the physical and chemical interactions involved during O₂ dissociation and oxygen incorporation into silicon, and is essential to establishing the relationship between processing conditions and actual oxide structure formation.

The paper gives an insight into the understanding of oxidation nucleation. Starting with O₂ chemisorption on Si(100)

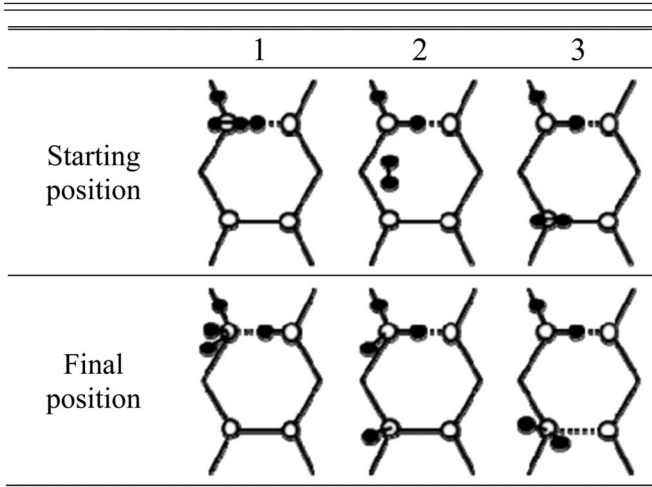
at different coverages, we focus on the identification and formation of the first oxide nucleus, where full oxygen incorporation becomes possible. It is shown that this process requires the local presence of two molecules. The overall mechanistic pathway for nucleation is based on the recognition that (i) the silanone structure, O=Si–O–Si, is the most stable structure for *single* O₂ chemisorption¹⁸ and (ii) two O₂ molecules are necessary to achieve full oxygen incorporation into the Si network (formation of Si–O–Si bonds). The calculations clearly show that this oxide seed, kinetically and thermodynamically favorable, with fully incorporated oxygen, is semihexagonal (SH) (noncubic) on the cubic substrate, clearly pointing to a subsequent pathway for the oxide amorphization.

Recently, a joint experimental [scanning tunnel microscope (STM) and IR spectroscopies] and theoretical investigation¹⁸ has explained the propensity of a single oxygen molecule to remain on top of the silicon surface, whether it is dissociated or not, without full oxygen incorporation. A resulting Si=O “strand” is remarkably stable until more oxygen can migrate and agglomerate. By bringing a second O₂ molecule in the vicinity of an existing silanone species, the local oxidation process can be investigated without the complications of oxygen diffusion (i.e., room-temperature oxidation),¹⁹ thus highlighting the mechanism for oxygen incorporation-induced structural rearrangements.

II. COMPUTATIONAL DETAILS

Calculations are performed with the plane-wave package VASP (Ref. 20) in the framework of the density functional theory (DFT) using the generalized gradient approximation and ultrasoft pseudopotentials²¹ to describe the silicon, hydrogen, and oxygen atoms. The unit cell is composed of a six-layer slab with eight atoms per layer and H termination of the bottom surface (Si₄₈H₁₆). The energy cutoff is fixed at 475 eV for basis set expansions. Due to the large size of our

TABLE I. Top view of starting positions and final configurations for the adsorption process of an O_2 molecule on a silanone containing oxidized surface. Atoms of oxygen are in black and atoms of Si are in white.



supercell (i.e., 17.9, 10.8, and 10.8 Å), the Brillouin zone is sampled at the Γ point which is shown to offer reasonable compromise for a qualitative structural/energetic based study.^{15,18,22,23} The spin polarization is taken into account in the calculations in order to describe adequately the oxygen molecule and its spin modifications.^{13,15,17} The eight surface atoms are $p(2 \times 2)$ reconstructed with four alternating tilted dimers, with one channel between two-dimer rows. A vacuum zone of 10 Å is placed between each slab in the z direction to create a surface. The sixteen silicon atoms of the two bottom layers of the slab and the passivating hydrogen atoms are kept fixed in order to mimic the bulk material. All other atoms are free to relax. The relaxation is performed using the conjugate gradient method. The energy barriers have been calculated using the nudged elastic band method (NEB).²⁴

III. THEORETICAL RESULTS

The starting point of our calculations considers a preoxidized silicon surface containing the silanone structure¹⁸ obtained after adsorption of one O_2 molecule as shown in Table I. The formation of this silanone is calculated to weaken both the dimer bond and the backbonds of the silicon atom of the dimer adjacent to that containing the silanone structure (data not shown). This implies that the lowest barriers for further O_2 dissociation will involve these three bonds. Given this situation, three locations were considered for O_2 approach onto the surface, summarized in the top row of Table I: the oxygen molecule is placed above the silanone structure (number 1), between the two adjacent dimer units (number 2), and above the most weakened silicon atom, on the adjacent dimer (number 3). The resulting coverage after dissociating two O_2 molecules on our unit cell is 0.5. For all three cases, we find that the oxygen molecule chemisorbs without incorporation of any oxygen atom in the Si-Si bonds, similarly to the case of a single oxygen molecule reacting with

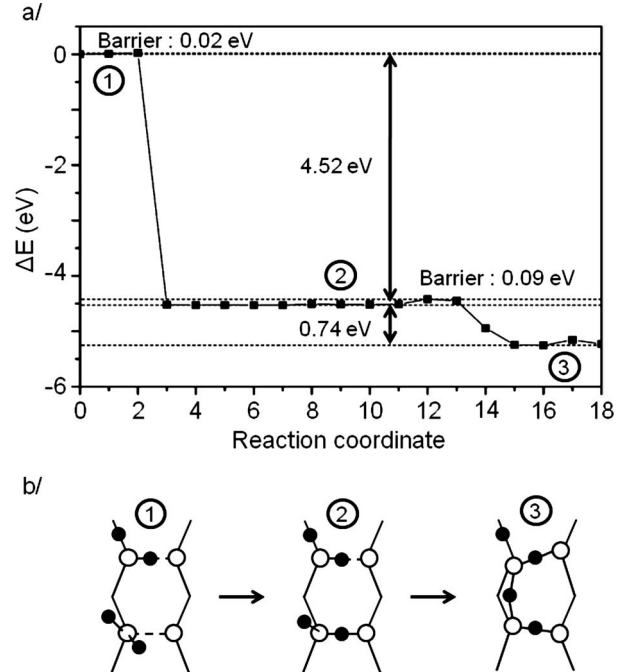


FIG. 1. (a) Energy pathway for oxygen incorporation from the structure shown as 3 in Table I (bottom row). Energy (in eV) is plotted versus reaction coordinates. (b) Reduced slab structures composed of two-dimer units are given at the main steps of the reaction pathway from the starting configuration 1 into the stable SH structure shown in 3. The atoms of oxygen are in black and atoms of Si are in white.

the silicon surface.^{15,18} In case 2, there is a complete dissociation leading to a large energy gain (~ 5 eV) while for cases 1 and 3, the molecule is not fully dissociated with both oxygen atoms attached to one Si surface atom resulting in a lower energy gain (~ 2 eV). Given these relatively large energy gains, the adsorption activation barriers (~ 0.02 eV) are negligible. As previously observed for one O_2 molecule adsorption,¹⁸ there is a propensity for oxygen to remain on top in a strand configuration (Si=O), giving to the O atoms the mobility to migrate into the lowest energy preincorporation geometries. Given this observation, most insight into oxygen incorporation can be gained by starting with configuration 3 (Table I) because there are more options for dissociation pathways. Indeed, position 2 is more limited because the molecule is already fully dissociated. Along the same line, position 1 requires more oxygen migration steps toward an oxygen-free Si-Si bond of one neighboring dimer unit before an additional incorporation mechanism is possible.

Figure 1(a) shows the calculated pathways and associated energies for oxygen incorporation starting from configuration 3. One of the two oxygen atoms is found to incorporate into the Si-Si dimer bond [Fig. 1(b), structure 2], with a net energy gain of 4.52 eV and negligible barrier (~ 0.02 eV). At this step, three migration pathways are possible for the remaining strand oxygen atom: (i) two involving the incorporation into the cubic Si lattice, i.e., toward the two Si-Si backbonds of the dimer unit, and (ii) one in an adjacent dimer bridging site (ADB). This last ADB configuration has been described in Refs. 15 and 23 and is characterized as an

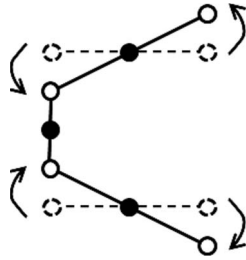


FIG. 2. Schematics illustrating the transition from perfectly aligned dimer units within the dimer row (dash lines) into tilted dimer units (full lines) initiating a SH pattern at the Si/SiO₂ interface. The atoms of oxygen are in black and atoms of Si are in white.

oxygen atom forming a Si–O–Si bridge between two adjacent dimer units perpendicular to the dimer bonds (referred to as “a surface bridging oxygen” in Yamasaki’s work¹²). From thermodynamic considerations, the ADB sites are important to stabilize high coverage layers [>1 monolayer (ML)].

The migration pathway toward the ADB configuration is therefore considered first, resulting in structure 3 in Fig. 1(b). The activation barrier is found to be very small (0.09 eV), negligible compared to previous gains of energy (2.16 and 4.52 eV). This oxygen incorporation step leads to an additional energy gain of 0.74 eV for a total exothermicity as large as 7.42 eV for the full O₂ adsorption/dissociation/incorporation process. The activation barrier for this second oxygen atom migration (0.09 eV) is strikingly low in view of typical surface diffusion barriers for single oxygen atoms (~ 0.9 eV),²² and is due to the large charge transfers arising from the local agglomeration of incorporated oxygen atoms as previously seen in Refs. 23 and 25. In particular, as the ADB configuration is formed during this last step, the oxygen atom belonging to the Si=O strand of the original silanone is fully incorporated into the dimer, facilitating the migration of the second Si=O strand into the ADB site. The initial silanone loss is operated during the chemisorption process of the second approaching O₂ molecule in 1. While in 3, the silanone configuration vanishes as ADB is formed (1.59–1.74 Å original asymmetry of Si=O–Si on dimer containing the silanone structure becomes almost symmetrical: 1.69–1.64 Å).

The energetically favorable incorporation of the overall process (0.74 eV for the last step with a 0.09 eV activation barrier) is in contrast to the difficulty (~ 0.15 eV endothermic process with a 0.63 eV activation barrier) of the Si=O strand of a single silanone to incorporate into the Si–Si network.¹⁸ This underscores the dependence of oxygen incorporation on the surface coverage.

The ADB structure is not an expected configuration for the cubic Si(100) surface because it requires two processes that should cost energy: (i) the rotation of the dangling bonds by a full 90° angle, and (ii) the distortion of the two adjacent dimers. Its calculated stability suggests that, even at 0.5 ML, a fundamental transition is taking place between the Si cubic symmetry (Fig. 2 dashed lines) and the preferred oxide structure involving a SH pattern (Fig. 2 full lines). This SH pattern, in agreement with the experimental observation by

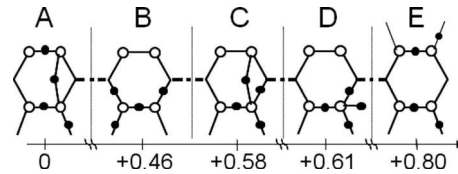


FIG. 3. Relative stability (in eV) of various dimer units containing four oxygen atoms inserted into the surface silicon layer, using the most stable as reference. The atoms of oxygen are in black and atoms of Si are in white.

Ourmazd⁶ that a tridymite structure is to be considered at the interface, is also consistent with the experimental observations of isolated nuclei formed at the primary stages of the oxidation process.^{26–28} The SH pattern constitutes the necessary template for an amorphous SiO₂ network (with local ring structures) to be formed.

To rigorously test that this SH pattern is thermodynamically preferred, all the possible structures associated with one, two, three, and four oxygen atoms have been calculated. For instance, Fig. 3 shows the five possible structures for four atoms. The SH structure (configuration A in the Fig. 3) is 0.46 eV more favorable than the systematic incorporation of all four oxygen atoms within a *single* dimer unit (configuration B). The results point to the competition between the energy gain resulting from oxygen atoms agglomeration (compare B and E, and D and E) and the role of the ADB bond configuration in distributing the oxygen atoms over the two-dimer units (compare C and A).

The SH structure is qualitatively different from any other low energy structure involving fully inserted oxygen atoms because it exhibits primarily Si–O–Si bonds, which maximizes second-nearest neighbors (two-dimer bonds and one ADB). All the other structures involve more nearest-neighbor-inserted oxygen atoms. The stabilization of oxygen atoms widely distributed over the two-dimer units is a unique property of the SH structure. Thus, early in the oxidation process, the oxide imposes its ringlike structure even at coverages as low as 0.5 ML. Interestingly, the SH structure also minimizes the number of dangling bonds within the unit cell, compared to all the other structures (0.5 ML in the present case), and is characterized by the only dangling-bond-free Si³⁺ species, typically observed in the substoichiometric interfacial layer shown in x-ray photoemission spectroscopy (XPS) experiments.^{29–31} These are two critical elements that characterize a full Si/SiO₂ interface.

If instead of forming a SH structure [Fig. 3(a)], oxygen atoms are forced into the existing Si–Si bonds [i.e., within the cubic structure, Fig. 3(b)], then there is a net energy cost of 0.46 eV at that coverage (0.5 ML). On the other hand, the formation of an ADB bond at lower coverages may not be favorable. Indeed, if only one oxygen atom is considered in the eight Si atom unit cell, the energy of the ADB is 1.5 eV higher than that in the insertion into a backbond.²² This observation indicates that the distortion of the two dimers is unfavorable without other oxygen atoms inserted in backbonds. Moreover, this distortion induced by tilted dimer units agrees well with previous theoretical investigations, offering the possibility to an additional oxygen molecule to diffuse in

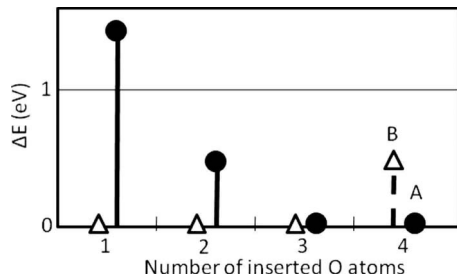


FIG. 4. Relative energies (in eV) of oxidized structures as a function of the number of oxygen atoms (from one to four) inserted into Si(100), using the most stable configuration as the energy reference. Open triangles correspond to oxygen incorporated fully into Si-Si bonds, and dark circles to the most stable structures containing ADB.

its molecular form through the interfacial layer and to penetrate the silicon substrate to pursue the oxidation process at the interface.^{5,32}

This SH pattern structure is shown to induce strain effect in the silicon layer immediately connected to it underneath. Indeed, the silicon atoms below the SH configuration were brought down from their initial crystalline silicon positions. We found a global piling up of the silicon layers as follows: around 0.7 Å for the first silicon layer connected to the SH, and around 0.3 and 0.1 Å for the second and the third submonolayer, respectively. The SH pattern influence therefore propagates from the interface down to the third sublayer of the silicon substrate below the interface as observed in Ref. 33 for a complete oxide coverage of the substrate. Of course, the extrapolation of the SH structure to obtain a full coverage of the substrate and its subsequent relation with defect generation is to be considered with much care. The real interface, involving many layers of oxide, involves also many specific basic mechanisms beyond the one discussed here for nucleation (oxygen diffusion for instance). However, if not direct, the atomic arrangement of the SH and silicon atoms connected to it are consistent with interfaces observed experimentally^{34–36} and associated phenomena that are known to lead to defect generation.³⁷

Figure 4 summarizes the results for one through four oxygen atoms arranged either in the most stable structures containing at least one ADB site or in the most stable structures without ADB sites. In both cases, numerous structures were considered and only the lowest energy configuration is selected. The absolutely lowest energy configuration is chosen as zero of the energy to highlight the energy difference be-

tween the ADB-containing structures and the others. The results for intermediate coverages (two and three oxygen atoms in the unit cell) show that the break even point is with three oxygen atoms, for which the ADB and Si-Si inserted positions give comparable energies. With only one oxygen atom inserted in the silicon,²² the energetic difference between the most stable configuration, which is a backbond oxidation, and an ADB conformation is 1.46 eV. For two oxygen atoms as described in Ref. 18, the 2-O atom structure containing the ADB characteristic, composed by one oxygen atom inserted into a backbond in addition to the ADB oxygen atom, is less stable by 0.46 eV than the most stable structure referred to as the silanone.

IV. CONCLUSIONS

In conclusion, DFT calculations have shown that, at coverages when the interaction of each O₂ molecule remains isolated from other oxygen species, the most stable structures emphasize a silanone configuration characterized by Si=O strands. The presence of Si=O underscores the difficulty for oxygen to fully incorporate into the cubic Si lattice. In general at higher temperatures, there is a propensity for oxygen to agglomerate within a single dimer unit, involving Si-O-Si bonds of nearest-neighbor units.³⁸ A remarkable transition takes place even at low temperatures when the coverage is increased from $\frac{1}{4}$ to $\frac{1}{2}$ ML. This transition, involving the interaction of two O₂ molecules, involves a fundamental configuration characterized by an adjacent dimer bridging bond that initiates a SH structure directly on the cubic Si substrate. While this SH geometry is reminiscent of the tridymite structure, the lattice mismatch between a hexagonal tridymite and cubic silicon (~11%) leads to the amorphization of the interface and the subsequently grown oxide. Studies of coverages higher than 0.5 ML will clarify the point at which strain will lead to disorder, but the essential element for symmetry transition is this quasibarrierless formation of the SH structure. Along this line, the recent work by Buczko *et al.*³⁹ opens exciting directions for the present study, i.e., extension of the SH nucleus: equilibrium structures are compared and tridymitelike configuration are shown to be favored.

This work also provides the basis for understanding the substoichiometric layers present in typical thin native oxides (presence of Si³⁺, absence of dangling bonds, and quasilocated order). More generally, the silicon oxidation provides a model system to understand complex crystalline/amorphous abrupt interfaces. Unraveling the mechanism for SH formation on a cubic lattice opens the door to understanding more complex materials such as SiGe, SiC, Ge, III-V semiconductors, and possibly carbon-based materials (graphene).

*chabal@utdallas.edu

¹S. C. Witzak, J. S. Suehle, and M. Gaitan, *Solid-State Electron.* **35**, 345 (1992).

²A. Stesmans and V. V. Afanas'ev, *J. Phys.: Condens. Matter* **10**, L19 (1998).

³M. T. Bohr, R. S. Chau, T. Ghani, and K. Mistry, *IEEE Spectrum* **44**, 29 (2007).

⁴A. Pasquarello, M. S. Hybertsen, and R. Car, *Nature (London)* **396**, 58 (1998).

⁵A. M. Stoneham, J. L. Gavartin, and A. L. Shluger, *J. Phys.: Condens. Matter* **17**, S2027 (2005).

⁶A. Ourmazd, D. W. Taylor, J. A. Rentschler, and J. Bevk, *Phys. Rev. Lett.* **59**, 213 (1987).

⁷G. Renaud, P. H. Fuoss, A. Ourmazd, J. Bevk, B. S. Freer, and P.

- O. Hahn, Appl. Phys. Lett. **58**, 1044 (1991).
- ⁸F. R. McFeely, K. Z. Zhang, M. M. Banaszak Holl, S. Lee, and J. E. Bender IV, J. Vac. Sci. Technol. B **14**, 2824 (1996).
- ⁹D. A. Muller and G. D. Wilk, Appl. Phys. Lett. **79**, 4195 (2001).
- ¹⁰A. Pasquarello, M. S. Hybertsen, and R. Car, Phys. Rev. Lett. **74**, 1024 (1995).
- ¹¹K.-O. Ng and D. Vanderbilt, Phys. Rev. B **59**, 10132 (1999).
- ¹²T. Yamasaki, K. Kato, and T. Uda, Phys. Rev. Lett. **91**, 146102 (2003).
- ¹³K. Kato and T. Uda, Phys. Rev. B **62**, 15978 (2000).
- ¹⁴Y. Miyamoto and A. Oshiyama, Phys. Rev. B **41**, 12680 (1990).
- ¹⁵A. Hemeryck, N. Richard, A. Estève, and M. Djafari Rouhani, J. Non-Cryst. Solids **353**, 594 (2007).
- ¹⁶Y. Widjaja and C. B. Musgrave, J. Chem. Phys. **116**, 5774 (2002).
- ¹⁷X. L. Fan, Y. F. Zhang, W. M. Lau, and Z. F. Liu, Phys. Rev. Lett. **94**, 016101 (2005).
- ¹⁸A. Hemeryck, A. J. Mayne, N. Richard, A. Estève, Y. J. Chabal, M. Djafari Rouhani, G. Dujardin, and G. Comtet, J. Chem. Phys. **126**, 114707 (2007).
- ¹⁹M. Ramamoorthy and S. T. Pantelides, Phys. Rev. Lett. **76**, 267 (1996).
- ²⁰G. Kresse and J. Furthmüller, Phys. Rev. B **54**, 11169 (1996); G. Kresse and D. Joubert, *ibid.* **59**, 1758 (1999).
- ²¹D. Vanderbilt, Phys. Rev. B **41**, 7892 (1990).
- ²²A. Hemeryck, N. Richard, A. Estève, and M. Djafari Rouhani, Surf. Sci. **601**, 2339 (2007).
- ²³A. Hemeryck, N. Richard, A. Estève, and M. Djafari Rouhani, Surf. Sci. **601**, 2082 (2007).
- ²⁴G. Mills, H. Jonsson, and G. K. Schenter, in *Classical and Quantum Dynamics in Condensed Phase Simulations*, edited by B. J. Berne, G. Cicciotti, and D. F. Coker (World Scientific, Singapore, 1998), p. 385.
- ²⁵A. Estève, M. Djafari Rouhani, and D. Estève, Comput. Mater. Sci. **24**, 241 (2002).
- ²⁶T.-W. Pi, J.-F. Wen, C.-P. Ouyang, R.-T. Wu, and G. K. Wertheim, Surf. Sci. **478**, L333 (2001).
- ²⁷N. Miyata, H. Watanabe, and M. Ichikawa, Phys. Rev. B **58**, 13670 (1998).
- ²⁸D. Hojo, N. Tokuda, and K. Yamabe, Thin Solid Films **515**, 7892 (2007).
- ²⁹F. J. Himpsel, F. R. McFeely, A. Taleb-Ibrahimi, J. A. Yarmoff, and G. Hollinger, Phys. Rev. B **38**, 6084 (1988).
- ³⁰F. Rochet, C. Poncey, G. Dufour, H. Roulet, C. Guillot, and F. Sirotti, J. Non-Cryst. Solids **216**, 148 (1997).
- ³¹J. H. Oh, H. W. Yeom, Y. Hagimoto, K. Ono, M. Oshima, N. Hirashita, M. Nywa, A. Toriumi, and A. Kakizaki, Phys. Rev. B **63**, 205310 (2001).
- ³²A. Bongiorno and A. Pasquarello, J. Phys.: Condens. Matter **17**, S2051 (2005).
- ³³A. Bongiorno, A. Pasquarello, M. S. Hybertsen, and L. C. Feldman, Phys. Rev. Lett. **90**, 186101 (2003).
- ³⁴S. D. Kosowsky, P. S. Pershan, K. S. Krisch, J. Bevk, M. L. Green, D. Brasen, L. C. Feldman, and P. K. Roy, Appl. Phys. Lett. **70**, 3119 (1997).
- ³⁵S. Dreiner, M. Schürmann, M. Krause, U. Berges, and C. Westphal, J. Electron Spectrosc. Relat. Phenom. **144-147**, 405 (2005).
- ³⁶A. Bongiorno, A. Pasquarello, M. S. Hybertsen, and L. C. Feldman, Phys. Rev. B **74**, 075316 (2006).
- ³⁷C. K. Ong, A. H. Harker, and A. M. Stoneham, Interface Sci. **1**, 139 (1993).
- ³⁸M. K. Weldon, K. T. Queeney, Y. J. Chabal, B. B. Stefanov, and K. Raghavachari, J. Vac. Sci. Technol. B **17**, 1795 (1999).
- ³⁹R. Buczko, S. J. Pennycook, and S. T. Pantelides, Phys. Rev. Lett. **84**, 943 (2000).